

# Asymptotic expressions for the angular dependence of low-frequency pulsation modes in rotating stars

R. H. D. Townsend<sup>★</sup>

*Department of Physics & Astronomy, University College London, Gower Street, London WC1E 6BT*

Accepted 2002 December 17. Received 2002 December 16; in original form 2002 September 25

## ABSTRACT

Through the solution of Laplace’s tidal equations, approximated to describe equatorially trapped wave propagation, analytical expressions are obtained for the angular dependence of pulsation modes in uniformly rotating stars. As the ratio between rotation and pulsation frequencies becomes large, these expressions approach the exact solutions of the governing low-frequency pulsation equations.

Four classes of asymptotic solution are found, corresponding to *g* (gravito-inertial), *r* (Rossby), Kelvin and Yanai modes. The Kelvin modes arise through the conservation of specific vorticity, much like the *r* modes, but propagate in the same sense as the rotation; they are found to be the equivalents of prograde sectoral modes. The prograde Yanai modes behave like *g* modes, as do the retrograde ones if the rotation is sufficiently rapid; otherwise, the latter exhibit the character of *r* modes.

Comparison between asymptotic and numerical solutions to the tidal equations reveals that the former converge rapidly towards the latter, for *g* and Yanai modes. The convergence is slower for Kelvin and *r* modes, as these become equatorially trapped only when the rotation is very rapid. It is argued that the utility of the asymptotic solutions does not rest on their accuracy alone, but also on the valuable physical insights that they are capable of providing.

**Key words:** hydrodynamics – waves – methods: analytical – stars: oscillations – stars: rotation.

## 1 INTRODUCTION

The past 15 years’ research into non-radial pulsation (nrp) in rotating stars have seen many qualitative insights obtained through the adoption of the so-called ‘traditional approximation.’ Originating from the field of atmospheric and oceanographic geophysics (Eckart 1960), this approximation was first applied in an astrophysical context by Lee & Saio (1987), to analyse the influence of the Coriolis force on low-frequency modes within massive, uniformly rotating stars. It has subsequently been applied in many areas of stellar pulsation, from modelling the nrp-originated line-profile variations seen in early-type stars (Lee & Saio 1990; Townsend 1997b), to examining tidal forcing in massive binary systems (Papaloizou & Savonije 1997), to investigating what role gravity modes might play in the quasi-periodic oscillations exhibited by rotating neutron stars (Bildsten, Ushomirsky & Cutler 1996).

Under the condition that a star is rotating with uniform angular velocity  $\Omega$ , the traditional approximation amounts to neglecting the horizontal component of  $\Omega$  when evaluating the inertial Coriolis force in the linearized momentum equations. Such an approach is valid in regions of the star where both  $\Omega \equiv |\Omega|$  and  $\omega$ , the pulsation

angular frequency in the corotating frame, are significantly smaller than the Brunt–Väisälä frequency  $N$  (see, e.g. Lee & Saio 1997). When combined with three other simplifying assumptions, namely

(i) that  $\Omega \ll (GM/R^3)^{1/2}$ , where  $M$  and  $R$  are the mass and radius of the star, respectively, such that centrifugal distortion of the quiescent star may be neglected,

(ii) that perturbations to the specific entropy may be neglected (the adiabatic approximation) and

(iii) that perturbations to the gravitation potential may be neglected [the Cowling (1941) approximation],

the traditional approximation permits the separation of the pulsation equations in all three spherical-polar coordinates ( $r$ ,  $\theta$ ,  $\phi$ ). This represents a great simplification, by transforming the nature of the problem from a partial differential one into an ordinary differential one.

Of the separated pulsation equations, that describing the azimuthal ( $\phi$ ) dependence of modes is the same as in the case without rotation, and is trivial to solve. The polar ( $\theta$ ) dependence is governed by Laplace’s tidal equations (Bildsten et al. 1996), whose eigensolutions – satisfying the appropriate boundary conditions – are named after their originator, Hough (1898). The Hough functions constitute a one-parameter family in the ‘spin parameter’  $\nu \equiv 2\Omega/\omega$ ; associated with each is an eigenvalue  $\lambda$ , which is related to the

<sup>★</sup>E-mail: rhdt@star.ucl.ac.uk

effective horizontal wavenumber  $k_{\perp}$  of the pulsation via  $k_{\perp}^2 = \lambda/r^2$  (e.g. Townsend 2000). Although this latter expression suggests that  $\lambda$  must be positive, negative values can also arise, and are identified with convective modes stabilized by the Coriolis force (see Lee & Saio 1986). Such modes are not considered in the present work, and it is therefore assumed throughout that  $\lambda$  is positive.

At general values of the spin parameter  $\nu$ , the solution of Laplace's tidal equations must be approached numerically. However, as the present paper will demonstrate, approximate analytical solutions may be obtained that become exact in the asymptotic limit of large  $|\nu|$ . This result is well-established in the geophysical literature (see, e.g. Longuet-Higgins 1968; Gill 1982), but has yet to be applied to stellar nrp. The format of the paper is as follows. The following section reviews briefly the derivation of Laplace's tidal equations; in Section 3, approximations are then made to permit derivation of analytical solutions to the equations. These are classified in Section 4, and compared against numerical solutions to the tidal equations in Section 5. A summary of the main results of the paper then follows in Section 6.

## 2 LAPLACE'S TIDAL EQUATIONS

In a uniformly rotating star, and under the assumptions (i)–(iii) given in the preceding section (but not yet adopting the traditional approximation), the linearized equations governing nrp may be written, in the corotating frame, as

$$-\rho\omega^2\xi_r - 2i\rho\omega\Omega \sin\theta\xi_{\theta} = -\frac{\partial p'}{\partial r} - g\rho', \quad (1)$$

$$-\rho\omega^2\xi_{\theta} - 2i\rho\omega\Omega \cos\theta\xi_{\phi} = -\frac{1}{r}\frac{\partial p'}{\partial\theta}, \quad (2)$$

$$-\rho\omega^2\xi_{\phi} + 2i\rho\omega\Omega \cos\theta\xi_{\theta} + 2i\rho\omega\Omega \sin\theta\xi_r = -\frac{1}{r\sin\theta}\frac{\partial p'}{\partial\phi}, \quad (3)$$

$$\rho' + \frac{1}{r^2}\frac{\partial}{\partial r}(\rho r^2\xi_r) + \frac{\rho}{r\sin\theta}\frac{\partial}{\partial\theta}(\sin\theta\xi_{\theta}) + \frac{\rho}{r\sin\theta}\frac{\partial\xi_{\phi}}{\partial\phi} = 0, \quad (4)$$

and

$$\frac{\rho'}{\rho} = \frac{1}{\Gamma_1}\frac{p'}{p} + \xi_r\frac{N^2}{g} \quad (5)$$

(e.g. Lee & Saio 1997). Here,  $(\xi_r, \xi_{\theta}, \xi_{\phi})$  are the  $(r, \theta, \phi)$  components of the fluid displacement vector  $\xi$ ;  $p$  is the pressure;  $\rho$  is the density;  $g$  is the gravitational acceleration; and  $\Gamma_1 \equiv (\partial \ln p / \partial \ln \rho)_{\text{ad}}$  is the first adiabatic exponent. The prime ( $'$ ) denotes the Eulerian perturbation of the indicated quantity, and a periodic time-dependence proportional to  $e^{i\omega t}$  has been assumed for the pulsation.

Equations (1) and (3) each contain terms proportional to  $\Omega \sin\theta$ , arising from the horizontal component of the rotation angular velocity vector  $\Omega$ . These terms are discarded within the traditional approximation, leading to

$$-\rho\omega^2\xi_r = -\frac{\partial p'}{\partial r} - g\rho', \quad (6)$$

and

$$-\rho\omega^2\xi_{\phi} + 2i\rho\omega\Omega \cos\theta\xi_{\theta} = -\frac{1}{r\sin\theta}\frac{\partial p'}{\partial\phi}, \quad (7)$$

respectively. It is this modification which permits the separation of the pulsation equations (2) and (4)–(7) in all three coordinates. The general form of solutions is readily found by inspection. Together, equations (5) and (6) indicate that  $\xi_r$ ,  $p'$  and  $\rho'$  share the same polar dependence. Likewise, equations (2), (4) and (7) require that  $\xi_{\theta}$  and  $\xi_{\phi}$  share the same radial dependence. Finally, the fact that all equations are homogeneous and first-order in  $\phi$  leads to an  $e^{im\phi}$  azimuthal

dependence, where – in order to preserve the single-valued quality of solutions under the transformation  $\phi \rightarrow \phi + 2\pi$  – the azimuthal order  $m$  is constrained to integral values. The sign of  $m$  and of the spin parameter  $\nu$  combine to determine the propagation direction of a mode in the corotating reference frame:  $m\nu < 0$  corresponds to prograde, and  $m\nu > 0$  to retrograde, with axisymmetric modes having  $m = 0$ .

Taking all of these points into consideration, general solutions may be written as

$$\xi_r = Y_r(r)\Theta(\theta)e^{i(m\phi+\omega t)}, \quad (8)$$

$$p' = Y_p(r)\Theta(\theta)e^{i(m\phi+\omega t)}, \quad (9)$$

$$\rho' = Y_{\rho}(r)\Theta(\theta)e^{i(m\phi+\omega t)}, \quad (10)$$

$$\sin\theta\xi_{\theta} = Y_{\perp}(r)\hat{\Theta}(\theta)e^{i(m\phi+\omega t)}, \quad (11)$$

$$i\sin\theta\xi_{\phi} = Y_{\perp}(r)\tilde{\Theta}(\theta)e^{i(m\phi+\omega t)}, \quad (12)$$

where the  $\sin\theta$  terms in the last two expressions have been introduced as a convenience, to simplify subsequent developments. The three functions  $\Theta(\theta)$ ,  $\hat{\Theta}(\theta)$  and  $\tilde{\Theta}(\theta)$ , describing the polar dependence of solutions, are identified with the Hough functions discussed in the preceding section [although it should be remarked that some authors – e.g. Lee & Saio (1997) – prefer to reserve the designation ‘Hough function’ for  $\Theta(\theta)$  alone].

Substituting the general solutions (8–12) into the pulsation equations leads to

$$-\rho\omega^2Y_r = -\frac{dY_p}{dr} - gY_{\rho}, \quad (13)$$

$$Y_{\perp} = \frac{1}{\rho\omega^2r}Y_p, \quad (14)$$

$$Y_{\rho} + \frac{1}{r^2}\frac{d}{dr}(\rho r^2Y_r) - \frac{\rho\lambda Y_{\perp}}{r} = 0, \quad (15)$$

$$\frac{Y_{\rho}}{\rho} = \frac{1}{\Gamma_1}\frac{Y_p}{p} + Y_r\frac{N^2}{g}, \quad (16)$$

for the radial functions  $Y_{\dots}$ , and

$$-\hat{\Theta} - \nu\mu\tilde{\Theta} = \mathcal{D}\Theta, \quad (17)$$

$$-\tilde{\Theta} - \nu\mu\hat{\Theta} = m\Theta, \quad (18)$$

$$\lambda(1 - \mu^2)\Theta - \mathcal{D}\hat{\Theta} + m\tilde{\Theta} = 0, \quad (19)$$

as the corresponding equations for the Hough functions, where  $\mu \equiv \cos\theta$ ,  $\nu$  is as defined in the preceding section, and the differential operator  $\mathcal{D}$  is introduced as

$$\mathcal{D} \equiv \sin\theta\frac{d}{d\theta} \equiv (1 - \mu^2)\frac{d}{d\mu}. \quad (20)$$

As little confusion can arise, the dependence of the radial functions on  $r$  alone, and of the Hough functions on  $\theta$  alone, has not been explicitly indicated. The eigenvalue  $\lambda$  appears in equations (15) and (19) as a separation constant; its significance was discussed previously in Section 1.

Equation (18) may be used to eliminate  $\tilde{\Theta}$  from equations (17) and (19), leading, after rearrangement, to

$$(\mathcal{D} - m\nu\mu)\Theta = (\nu^2\mu^2 - 1)\hat{\Theta}, \quad (21)$$

$$(\mathcal{D} + m\nu\mu)\hat{\Theta} = [\lambda(1 - \mu^2) - m^2]\Theta. \quad (22)$$

In combination with the algebraic relation (18), these constitute Laplace's tidal equations in a first-order form; the further elimination

of  $\hat{\Theta}$  leads to the second-order form favoured by Bildsten et al. (1996) and Lee & Saio (1997).

In the following section, it will be demonstrated how the tidal equations can be solved analytically in the asymptotic limit  $|\nu| \gg 1$ . Out of the continuum of possible solutions, only those which satisfy the appropriate boundary conditions shall be retained. For non-axisymmetric modes (i.e.  $m \neq 0$ ), these conditions amount to the requirement that solutions decay towards zero as the points  $\mu = \pm 1$  are approached; this ensures that the general solutions (8–12) are (as near as possible) single-valued at the stellar poles. For the axisymmetric modes, the same decay requirement is applied to the polar gradient of the solutions, to maintain the smoothness of the general solutions at the poles.

### 3 ASYMPTOTIC SOLUTIONS

The key to deriving asymptotic solutions to Laplace’s tidal equations (18) and (21)–(22) lies in noting that the spin parameter  $\nu$  always appears in product with the latitudinal coordinate  $\mu$ . Intuition suggests that, if the Hough functions are to remain finite in the limit of large  $|\nu|$ , these functions can differ appreciably from zero only over a narrow equatorial region of small  $|\mu|$ .

This supposition is lent support by numerical solutions of the tidal equations. Bildsten et al. (1996) demonstrated that, towards larger values of  $|\nu|$ , the Hough functions remain close to zero outside the interval  $|\mu| \lesssim |\nu|^{-1}$ . The possibility of such confinement was first recognized by Yoshida (1959), who originated the idea of a Coriolis-force originated ‘equatorial waveguide’ which prevents low-frequency waves from propagating towards high latitudes.

For equatorially trapped waves, the fact that  $\mu$  is small suggests that terms of the order of  $\mu^2$  in the tidal equations may be neglected, in comparison to those of the order of unity. Under this approximation, the differential operator  $\mathcal{D}$ , appearing on the left-hand side of equations (21)–(22), becomes

$$\mathcal{D} \approx \frac{d}{d\mu}. \quad (23)$$

To obtain corresponding approximate forms for the right-hand sides of these equations, it is necessary to consider two separate cases, depending on whether the eigenvalue  $\lambda$  is close, or otherwise, to  $m^2$ . The following subsections consider each case in turn, and obtain the appropriate solutions to the approximated tidal equations.

#### 3.1 The case when $\lambda \neq m^2$

Under the ab initio assumption that  $\lambda$  differs appreciably from  $m^2$ , the  $\mu^2$  term on the right-hand side of equation (22) may be neglected. The tidal equations then become

$$\left( \frac{d}{d\mu} - m\nu\mu \right) \Theta = (\nu^2\mu^2 - 1)\hat{\Theta}, \quad (24)$$

$$\left( \frac{d}{d\mu} + m\nu\mu \right) \hat{\Theta} = (\lambda - m^2)\Theta, \quad (25)$$

where  $\mathcal{D}$  has been replaced by its approximate form (23). Eliminating  $\Theta$  between this pair leads to a second-order differential equation for  $\hat{\Theta}$ ,

$$\frac{d^2\hat{\Theta}}{d\mu^2} + (m\nu - m^2 + \lambda - \lambda\nu^2\mu^2)\hat{\Theta} = 0. \quad (26)$$

By introducing the definitions

$$\sigma \equiv (L\nu)^{1/2}\mu, \quad (27)$$

$$L^2 \equiv \lambda \quad (28)$$

and

$$S \equiv \frac{m\nu - m^2 + L^2}{L\nu}, \quad (29)$$

this equation further simplifies to

$$\frac{d^2\hat{\Theta}}{d\sigma^2} + (S - \sigma^2)\hat{\Theta} = 0. \quad (30)$$

It is no coincidence that this latter equation bears a close resemblance to the time-independent Schrödinger equation for a quantum harmonic oscillator (e.g. Arfken 1970) – both describe wave propagation within a quadratic potential well, which in the present context corresponds to the equatorial waveguide discussed above.

Solution of equation (30), subject to the boundary conditions given previously, can only be achieved when  $S$  satisfies the relation

$$S = 2s + 1 \quad (31)$$

for the integer ‘meridional order’  $s \geq 0$ . The solutions are given by

$$\hat{\Theta}(\sigma) = H_s(\sigma)e^{-\sigma^2/2}, \quad (32)$$

where  $H_s$  is the Hermite polynomial of order  $s$ . From equations (18) and (25), corresponding expressions for the other two Hough functions follow immediately, as

$$\begin{aligned} \Theta(\sigma) &= \frac{(L\nu)^{1/2}}{L^2 - m^2} \\ &\times \left[ s \left( \frac{m}{L} + 1 \right) H_{s-1}(\sigma) + \frac{1}{2} \left( \frac{m}{L} - 1 \right) H_{s+1}(\sigma) \right] e^{-\sigma^2/2} \end{aligned} \quad (33)$$

and

$$\begin{aligned} \tilde{\Theta}(\sigma) &= m \frac{(L\nu)^{1/2}}{m^2 - L^2} \\ &\times \left[ s \left( \frac{L}{m} + 1 \right) H_{s-1}(\sigma) + \frac{1}{2} \left( \frac{L}{m} - 1 \right) H_{s+1}(\sigma) \right] e^{-\sigma^2/2}; \end{aligned} \quad (34)$$

here, extensive use has been made of the recurrence relations between Hermite polynomials (e.g. Abramowitz & Stegun 1964).

The parameter  $L$  appears explicitly both in the last two expressions, and in the definition (27) of the independent variable  $\sigma$ . It can be found by solving the characteristic equation

$$L^2 - \nu(2s + 1)L + (m\nu - m^2) = 0 \quad (35)$$

derived from eliminating  $S$  between equations (29) and (31). The resulting roots are given by

$$L = \frac{1}{2}\nu(2s + 1) \pm \frac{1}{2} \left[ \nu^2(2s + 1)^2 - 4(m\nu - m^2) \right]^{1/2}. \quad (36)$$

From this relation, the eigenvalue  $\lambda$  is readily found as

$$\begin{aligned} \lambda_{\pm} \equiv L^2 &= -(m\nu - m^2) + \frac{1}{2}\nu^2(2s + 1)^2 \\ &\times \left\{ 1 \pm \left[ 1 - \frac{4(m\nu - m^2)}{\nu^2(2s + 1)^2} \right]^{1/2} \right\}, \end{aligned} \quad (37)$$

which – via a non-vanishing, lowest-order Taylor’s series expansion in  $\nu^{-1}$  – can be written in the approximate forms

$$\lambda_{\pm} \approx \nu^2(2s + 1)^2 + \mathcal{O}(\nu) \quad (38)$$

and

$$\lambda_- \approx \frac{(mv - m^2)^2}{v^2(2s + 1)^2} + \mathcal{O}(v^{-1}). \quad (39)$$

Each of these two eigenvalue branches is associated with a class of equatorially trapped wave/mode. The  $\lambda_+$  branch corresponds to gravito-inertial (g) modes (sometimes also known as Poincaré waves – see Gill 1982), which arise from the influence on displaced fluid elements of both buoyancy and Coriolis forces.

Likewise, the  $\lambda_-$  branch corresponds to r modes (or Rossby waves), which arise through the conservation of specific vorticity, combined with the curvature of level surfaces. Unlike the g modes, the r modes do not exist in non-rotating systems. The entire  $\lambda_-$  branch must be ruled out whenever  $mv \leq m^2$ , because the product  $Lv$  would otherwise be negative, and – via its definition (27) – the independent variable  $\sigma$  imaginary, which is inadmissible on physical grounds. An immediate corollary is that valid r-mode solutions, for which  $mv > m^2 \geq 0$ , are necessarily non-axisymmetric and retrograde; this is a well-established result (e.g. Saio 1982).

The foregoing discussion is applicable to both g and r modes of meridional order  $s \geq 1$ . The  $s = 0$  solutions comprise a special case, as their eigenvalues reduce to the exact forms

$$\lambda_+ = \begin{cases} m^2 & \text{when } 0 < mv < 2m^2, \\ (v - m)^2 & \text{otherwise,} \end{cases} \quad (40)$$

and

$$\lambda_- = \begin{cases} (v - m)^2 & \text{when } 0 < mv < 2m^2, \\ m^2 & \text{otherwise.} \end{cases} \quad (41)$$

The  $\lambda = m^2$  cases must be ruled out, because they violate the a priori assumption that  $\lambda$  differs appreciably from  $m^2$ . Furthermore, the remaining  $\lambda = (v - m)^2$  cases must be disallowed over the interval  $0 < mv < m^2$ , inasmuch that they arise from  $L = (v - m)$  solutions to the characteristic equation (35), and would therefore lead to imaginary values of  $\sigma$ . Accordingly, it can be seen that the  $s = 0$  situation leads to at most one valid solution, rather than the usual two. Where it exists, this solution has the character either of an r mode mode ( $\lambda = \lambda_-; m^2 < mv < 2m^2$ ), or a g mode ( $\lambda = \lambda_+; mv > 2m^2$  or  $mv \leq 0$ ), and for this reason it is sometimes termed the mixed gravity–Rossby wave (e.g. Gill 1982). In honour of its discovery in the Earth’s atmosphere by Yanai & Maruyama (1966), this wave is also known as the Yanai wave, and the present work will thus refer to the  $s = 0$  solutions as Yanai modes.

The accuracy of the asymptotic expressions (32–34) will be investigated in Section 5, through comparison with numerical solutions to the full tidal equations (18) and (21)–(22). Meanwhile, useful insights can be gleaned from consideration of  $\mu_{1/2}$ , the half-width of the equatorial waveguide. As the Hough functions reach appreciable amplitudes only within the waveguide, the error introduced by the asymptotic analysis – where terms of order  $\mu^2$  are neglected – should scale with  $\mu_{1/2}^2$ .

Of the alternative  $\mu_{1/2}$  definitions that might be adopted, a relatively simple one comprises the loci  $\mu = \pm\mu_{1/2}$  at which the  $\hat{\Theta}$  Hough function changes from oscillatory to exponential. These loci are where latitudinally propagating waves become evanescent, and can be considered reflected by the waveguide boundaries. From a mathematical stance, the loci can be identified as the points where  $\hat{\Theta}$  is non-zero, but its second derivative with respect to  $\mu$  vanishes. Under these conditions, equation (30) is satisfied only when  $\sigma^2 = S$ , leading to the expression

$$\mu_{1/2} = \left( \frac{2s + 1}{Lv} \right)^{1/2} \quad (42)$$

for the waveguide half-width. Through use of equation (28), and the approximate forms (38–39) for  $\lambda$ ,  $L$  may be eliminated from this result, to give

$$\mu_{1/2} \approx \frac{1}{|v|} \quad (43)$$

for the g modes, and

$$\mu_{1/2} \approx \left( \frac{2s + 1}{mv - m^2} \right)^{1/2} \quad (44)$$

for the r modes.

Recalling that the relative error varies with  $\mu_{1/2}^2$ , the former expression indicates that the g-mode solutions will converge approximately quadratically (in  $v$ ) to the exact solutions of the full tidal equations (18) and (21)–(22). In the case of the r modes, equation (44) reveals a closer-to-linear convergence, meaning that – for modest values of  $mv > m^2$  – these solutions will provide poor approximations to their exact counterparts. For both types of mode,  $\mu_{1/2}$  must clearly be less than unity if the notion of equatorial trapping is to hold any meaning; therefore, the g-mode solutions should be considered valid only when  $|v| \gtrsim 1$ , and the r-mode solutions only when  $mv \gtrsim 2s + 1 + m^2$ .

It should be remarked that Bildsten et al. (1996) adopt a different definition of the waveguide half-width, based on the outermost (i.e. largest- $|\mu|$ ) extremum in the  $\Theta$  Hough function. However, this definition led them to find the empirical relationship  $\mu_{1/2} \approx |v|^{-1}$ , the same as obtained above (cf. equation 43) for the g modes. The reason why the two alternative half-width definitions lead to the same expression for  $\mu_{1/2}$  can be understood by noting that, as the equatorial waveguide grows ever-more narrow, the  $\Theta$  Hough function necessarily becomes eclipsed in amplitude by its latitudinal derivative. Therefore, equation (24) may be approximated by

$$\frac{d\Theta}{d\mu} \approx (v^2\mu^2 - 1)\hat{\Theta}. \quad (45)$$

Clearly, the left-hand side will vanish (corresponding to a  $\Theta$  extremum) either when  $\mu = \pm v^{-1}$ , or when  $\hat{\Theta}$  is zero. The former situations can be identified with the outermost extrema of  $\Theta$ , by the simple argument that all zeros of  $\hat{\Theta}$  must lie equator-ward to  $\mu = \pm v^{-1}$  – these points, as shown above, being where  $\hat{\Theta}$  is non-zero, and its character changes from oscillatory to exponential. Therefore, it follows that the half-width definition adopted herein naturally leads to the same value of  $\mu_{1/2}$  predicted by the Bildsten et al. (1996) definition.

### 3.2 The case when $\lambda \approx m^2$

When  $\lambda$  is close to  $m^2$ , the solutions of the previous section do not apply, because the  $\mu^2$  term on the right-hand side of equation (22) cannot be discarded. However, because the whole bracketed term on this side will be small, it is reasonable to expect  $\Theta$  to be much larger in magnitude than  $\hat{\Theta}$ . With this assumption, the tidal equations may be approximated near the equator by

$$\left( \frac{d}{d\mu} - mv\mu \right) \Theta = 0, \quad (46)$$

$$\left( \frac{d}{d\mu} + mv\mu \right) \hat{\Theta} = [\lambda(1 - \mu^2) - m^2]\Theta, \quad (47)$$

where, as before,  $\mathcal{D}$  has been replaced by its approximate form (23). With a change of independent variable to

$$\tau \equiv (-m\nu)^{1/2} \mu, \quad (48)$$

the above equations become

$$\left( \frac{d}{d\tau} + \tau \right) \Theta = 0, \quad (49)$$

$$\left( \frac{d}{d\tau} - \tau \right) \hat{\Theta} = \frac{1}{(-m\nu)^{1/2}} \left[ \lambda - m^2 + \frac{\lambda\tau^2}{m\nu} \right] \Theta, \quad (50)$$

respectively. The first of these is solved trivially, to give

$$\Theta(\tau) = e^{-\tau^2/2}. \quad (51)$$

This solution can be identified with an equatorially trapped Kelvin wave (e.g. Gill 1982). Much like Rossby waves, Kelvin waves arise from the conservation of specific vorticity; however, it is the density stratification of the star, rather than its curvature, which is important in producing these waves. They propagate in a prograde rather than retrograde direction, which explains why they have been referred to in the astrophysical literature (see Unno et al. 1989) as low-frequency prograde waves. In the present context, the prograde nature of Kelvin waves can readily be seen from the requirement that  $\tau$  be real, and therefore that  $m\nu < 0$ .

The tangential ( $\hat{\Theta}$  and  $\tilde{\Theta}$ ) Hough functions associated with  $\Theta$  take a little more effort to obtain. Substituting solution (51) into equation (50) yields

$$\left( \frac{d}{d\tau} - \tau \right) \hat{\Theta} = \frac{1}{(-m\nu)^{1/2}} \left[ \lambda - m^2 + \frac{\lambda\tau^2}{m\nu} \right] e^{-\tau^2/2}, \quad (52)$$

which is readily rewritten as

$$\frac{d}{d\tau} \left( e^{-\tau^2/2} \hat{\Theta} \right) = \frac{1}{(-m\nu)^{1/2}} \left[ \lambda - m^2 + \frac{\lambda\tau^2}{m\nu} \right] e^{-\tau^2}. \quad (53)$$

Integrating the right-hand side by parts yields the general solution

$$\hat{\Theta}(\tau) = \frac{1}{(-m\nu)^{1/2}} \left[ \frac{\sqrt{\pi}}{2} \left( \lambda - m^2 + \frac{\lambda}{2m\nu} \right) e^{\tau^2/2} \text{erf}(\tau) - \frac{\lambda\tau}{2m\nu} e^{-\tau^2/2} \right] + T e^{\tau^2/2}, \quad (54)$$

where  $\text{erf}(\tau)$  is the error function, and  $T$  is a constant of integration. If the boundary conditions are to be satisfied,  $T$  must be set to zero, and the first term within the brackets must vanish, leading to the characteristic equation

$$\lambda = m^2 \frac{2m\nu}{2m\nu + 1}. \quad (55)$$

The solution for  $\hat{\Theta}$  reduces to

$$\hat{\Theta}(\tau) = -\frac{1}{(-m\nu)^{1/2}} \frac{m^2}{2m\nu + 1} \tau e^{-\tau^2/2}. \quad (56)$$

Via equation (18), this result can be combined with expression (51) for  $\Theta$ , to give the azimuthal Kelvin-mode Hough function as

$$\tilde{\Theta}(\tau) = -m \left( \frac{\tau^2}{2m\nu + 1} + 1 \right) e^{-\tau^2/2}. \quad (57)$$

Towards large  $|\nu|$ , the Kelvin-mode eigenvalues (55) asymptote towards  $m^2$ , and ever more closely satisfy the eigenvalue equation (37) when  $s = -1$ . Accordingly, Kelvin modes are sometimes attributed the notional meridional order  $s = -1$  (e.g. Gill 1982), a designation which will prove convenient when, in the following section, the solutions to the tidal equations are classified.

As in the preceding section, it is useful to determine the half-width  $\mu_{1/2}$  of the Kelvin-mode equatorial waveguide. The second

derivative of the  $\hat{\Theta}$  Hough function (56) vanishes at  $\tau = \pm\sqrt{3}$ ; therefore, through the definition (48) of  $\tau$ , the half-width follows as

$$\mu_{1/2} = \left( \frac{3}{-m\nu} \right)^{1/2}. \quad (58)$$

In the limit  $|\nu| \gg m^2$ , this expression predicts for the Kelvin modes the same linear- $\nu$  convergence found for the r modes, highlighting further the close relationship between the two.

#### 4 MODE CLASSIFICATION

In the preceding section, analytical expressions were obtained for the Hough functions, via solution of Laplace's tidal equations (18) and (21)–(22) in the limit of large  $|\nu|$ . Four types of equatorially trapped solution were found, corresponding respectively to g, r, Yanai and Kelvin modes. The purpose of the present section is to demonstrate how these relate to historical classifications of low-frequency nrp in rotating stars.

In the limit of no rotation, the  $\Theta$  Hough functions of all prograde modes, and of the retrograde g modes, reduce to associated Legendre functions  $P_\ell^m$  (Lee & Saio 1997); here,  $m$  is the usual azimuthal order, and the integer  $\ell \geq 0$  is the harmonic degree. The  $(\ell, m)$  pair of indices is often used to classify the Hough functions (e.g. Townsend 1997a,b), as it provides a clear indication of their non-rotating progenitors.

However, this classification scheme can encompass neither r modes, nor retrograde Yanai modes. To address this deficiency, an alternative scheme was devised by Lee & Saio (1997), centring around the assignment of a unique integer index  $k$  to each solution of the tidal equations. Positive or zero values of  $k$  indicate modes which possess a counterpart, of harmonic degree  $\ell = |m| + k$ , in the limit of no rotation; negative values denote the r modes and Yanai modes, or – when  $\lambda < 0$  – the convective modes neglected in the present analysis. The  $k$  indexing of solutions is determined by the requirement that the eigenvalues  $\lambda_k$ , at every  $m$  and  $\nu$ , fall into the sequence  $\lambda_{k+1} > \lambda_k$ . Such an ordering is always possible, because the eigenvalues of the tidal equation are guaranteed never to be degenerate (see, e.g. Townsend 1997a,b).

Using this stratagem, it is straightforward to relate the meridional order  $s$  of the solutions found herein to the  $k$  index of Lee & Saio (1997). For prograde modes, the correspondence takes the simple form  $s = k - 1$ , encompassing at a stroke the g modes ( $k \geq 2 \Leftrightarrow s \geq 1$ ), the Yanai mode ( $k = 1 \Leftrightarrow s = 0$ ) and the Kelvin mode ( $k = 0 \Leftrightarrow s = -1$ ). Likewise, the correspondence for retrograde modes is  $s = -k - 1$  for the r modes ( $k \leq -2 \Leftrightarrow s \geq 1$ ), and  $s = k + 1$  for the g modes ( $k \geq 0 \Leftrightarrow s \geq 1$ ); either one of these gives the correct relationship for the Yanai mode ( $k = -1 \Leftrightarrow s = 0$ ).

To clarify the foregoing exposition, Table 1 indicates how the  $m = -2, k = -2, \dots, 2$  modes fit into the  $s$ - and  $\ell$ -based indexing schemata. Also shown in the table is the type of each mode. Clearly, what has historically been designated as the prograde sectoral mode, with  $\ell = -m$ , can now be identified as an instance of a Kelvin mode; likewise, the lowest-order retrograde g mode can also be recognized as a sectoral mode ( $\ell = m$ ). However, the latter terminology is rather misleading: although, when  $|\nu| < 1$  the  $\Theta$  Hough functions of the  $\ell = m$  modes exhibit no latitudinal nodes over the range  $-1 < \mu < 1$ , an extra pair of nodes appears when  $|\nu|$  exceeds unity (e.g. Lee & Saio 1997). Therefore, in the limit of large  $|\nu|$ , the  $s = 1$  ( $k = 0$ ) retrograde g mode is not actually sectoral.

Comparing the alternative indexing schemes presented in Table 1, it can be seen that only the  $k$ -based one is capable of identifying all modes uniquely; the  $s$  scheme suffers from the drawback that,

**Table 1.** The correspondence between the  $k$ -based indexing scheme (Lee & Saio 1997) and the  $s$ - and  $\ell$ -based schemes, for prograde and retrograde  $m = -2$  modes. Situations where there is no valid index are denoted by ellipses (...).

$k$	Prograde ( $\nu > 0$ )			Retrograde ( $\nu < 0$ )		
	$s$	$\ell$	Mode type	$s$	$\ell$	Mode type
2	1	4	g	3	4	g
1	0	3	Yanai	2	3	g
0	-1	2	Kelvin	1	2	g
-1	...	...	...	0	...	Yanai
-2	...	...	...	1	...	r

without supplementary information, there is no way of distinguishing between g and r modes. However, it benefits from the fact that it provides a clear indication of the character of a given mode, which neither of the other schemes can achieve.

Equipped with the correspondence between the  $s$ ,  $k$  and  $\ell$  indexing schemes, it is straightforward to compare the results presented herein with those found by other authors. For instance, Lee & Saio (1997) have noted that  $l_\mu$ , the number of latitudinal nodes in  $\Theta$ , is given by  $l_\mu = k$  for prograde g modes, and by  $l_\mu = k + 2$  for retrograde g modes, the extra pair of nodes in the latter case appearing – as mentioned above – when  $|\nu| > 1$ . Expressed in the  $s$ -based scheme, this relationship becomes  $l_\mu = s + 1$  for both prograde and retrograde modes; therefore, the approximate expression (38) for  $\lambda_+$  may be written in terms of  $l_\mu$ , as

$$\lambda_+ \approx \nu^2(2l_\mu - 1)^2. \quad (59)$$

This is identical to the asymptotic behaviour found by (Bildsten et al. (1996, their equation 14); however, they arrived at their result empirically, in contrast to the analytical approach herein.

To provide another example, Lee & Saio (1989) have demonstrated, via asymptotic solution of the *radial* parts of the pulsation equations (cf. 13–16), that the eigenfrequencies of low-frequency g modes satisfy

$$\omega = \left(\frac{\lambda}{2}\right)^{1/2} \omega_1, \quad (60)$$

in the case of early-type stars with convective cores and radiative envelopes. The quantity  $\omega_1$  is the frequency of the  $\ell = 1$  mode of radial order  $n$  in a non-rotating star, defined as

$$\omega_1 = \frac{\sqrt{2}}{(\eta_e/2 + n)\pi} \int_{R_c}^R \frac{N}{r} dr, \quad (61)$$

where  $R_c$  is the radius of the core boundary, and  $\eta_e$  is the effective polytropic index at the stellar surface. Through use of the approximate form (38),  $\lambda$  may be eliminated from equation (60), to yield

$$\omega = \frac{\nu(2s + 1)\omega_1}{\sqrt{2}}. \quad (62)$$

Using the definition  $\nu \equiv 2\Omega/\omega$  of the spin parameter, and the above identification  $l_\mu = s + 1$ , the latter expression can also be written as

$$\omega^2 = \sqrt{2}(2l_\mu - 1)\Omega\omega_1. \quad (63)$$

In the limit  $l_\mu \gg 1$ , this result is in agreement with the findings of Papaloizou & Pringle (1978), in their study of equatorially trapped g modes (see also Ushomirsky & Bildsten 1998).

## 5 CALCULATIONS

In this section, the asymptotic solutions to the tidal equations (18) and (21)–(22) are compared with ‘exact’ numerical solutions. This comparison is not intended to be exhaustive, but rather to illustrate the validity and accuracy of the analysis presented in the foregoing sections. The technique adopted for calculation of the numerical solutions was Townsend’s (2003) implementation of the matrix-based formalism introduced by Lee & Saio (1990). Where appropriate, Hough functions were normalized using the approach of Lee & Saio (1997): those of even  $k$  were scaled so that  $\Theta = 1$  at  $\mu = 0$ , and those of odd  $k$  so that  $d\Theta/d\mu = 1$  likewise.

### 5.1 Eigenvalues

Fig. 1 shows the asymptotic [ $\lambda^{(a)}$ ] and numerical [ $\lambda^{(n)}$ ] Hough eigenvalues for  $m = -2$ ,  $k = -2, \dots, 2$  modes, plotted as a function of the spin parameter  $\nu$ . Each curve has been labelled with its  $k$  index, and the  $s$  index predicted by the correspondences discussed in the preceding section. In light of the fact that the asymptotic solutions are valid only when the waveguide half-width is less than unity (cf. Section 3.1), the  $\lambda^{(a)}$  data have not been plotted for  $\mu_{1/2} < 1$ ; throughout,  $\mu_{1/2}$  was determined using one of either equations (42) or (58).

From the figure, it is immediately clear that the  $\lambda^{(a)}$  curves approach the corresponding  $\lambda^{(n)}$  ones as  $|\nu|$  increases. This occurs most rapidly for the g modes; by  $|\nu| = 2$ , the differences between the two are already quite small. As anticipated by the analysis of Section 3.1, the convergence is much slower for the r mode ( $k = -2$ ). The Yanai mode ( $k = -1$ ) is an intermediate case, converging slowly at first, but more rapidly once its character switches towards that of a g mode.

To appreciate better the differences between the asymptotic and numerical eigenvalues, Fig. 2 plots the relative error

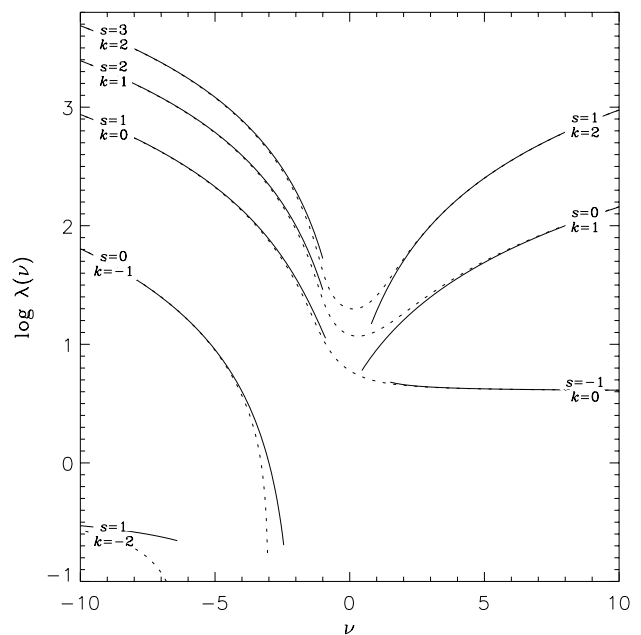


**Figure 1.** The asymptotic [ $\lambda^{(a)}$ ; solid] and numerical [ $\lambda^{(n)}$ ; dotted] eigenvalues for  $m = -2$ ,  $k = -2, \dots, 2$  modes, plotted as a function of the spin parameter  $\nu$ . Each pair of curves is labelled by the appropriate  $k$  and  $s$  indices.

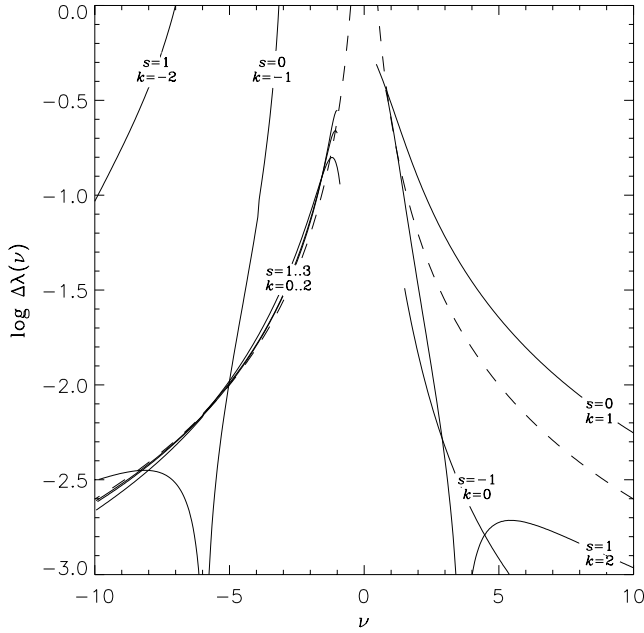


**Figure 2.** The relative error  $\Delta\lambda$  between asymptotic and numerical eigenvalues, plotted as a function of  $\nu$ , for  $m = -2$ ,  $k = -2, \dots, 2$  modes. Each curve is labelled by the appropriate  $k$  and  $s$  indices; the dashed line indicates the relation  $\Delta\lambda = (2\nu)^{-2}$ .

$$\Delta\lambda \equiv \left| \frac{\lambda^{(n)} - \lambda^{(a)}}{\lambda^{(n)}} \right| \quad (64)$$

as a function of the spin parameter. Also shown in the figure is the curve  $\Delta\lambda = (2\nu)^{-2}$ , which illustrates an interesting finding: that the relative error for the g modes ( $s \geq 1$ ) and the Kelvin wave ( $s = -1$ ) exhibits an approximate upper bound  $\Delta\lambda \approx (2\nu)^{-2}$ . The retrograde modes all lie quite close to this bound, whilst the prograde modes fall well below it with increasing  $\nu$ .

Supplementary calculations revealed such behaviour is not restricted to the modes plotted in Fig. 2, but applies also to (at least) the Kelvin and g modes of azimuthal orders  $0 \leq |m| \leq 8$ . It therefore appears reasonable to advance the empirically-driven hypothesis, that the error associated with such modes obeys  $\Delta\lambda \lesssim (2\nu)^{-2}$  *universally*. A corresponding hypothesis can be put forward regarding the prograde Yanai ( $s = 0$ ) mode; when  $\nu \gtrsim 3$ , the error in its case was found to follow  $\Delta\lambda \approx (4/3 \nu)^{-2}$  for the range of azimuthal orders indicated above. Interestingly, both of these hypotheses follow the  $\nu^{-2}$  error scaling predicted for g modes in the latter parts of Section 3.1.

## 5.2 Hough functions

Moving now to an examination of the Hough functions, Fig. 3 shows the  $\mu$ -dependence of both the asymptotic functions  $\{\Theta^{(a)}, \hat{\Theta}^{(a)}, \tilde{\Theta}^{(a)}\}$ , and their numerical counterparts  $\{\Theta^{(n)}, \hat{\Theta}^{(n)}, \tilde{\Theta}^{(n)}\}$ , for the  $m = -2$ ,  $k = -2, \dots, 2$  modes considered previously. The  $k \geq 0$  modes are shown at spin parameters  $\nu = \pm 3$ , while the  $k = -2, -1$  ones are considered only for  $\nu = -6$ , since they do not possess prograde counterparts. Each plot has been labeled with the  $s$  index corresponding to the appropriate value of  $k$ , and the location of the waveguide boundary at  $\mu = \mu_{1/2}$  – as dictated by equations (42) and (58) – has been indicated with a dashed vertical line.

For the g modes, the agreement between the asymptotic and numerical Hough functions is quite good. Generally speaking, the

greatest degree of discrepancy between the two sets of functions arises in the mid-latitudes ( $0.2 \lesssim \mu \lesssim 0.8$ ). This is because the approximations adopted for the asymptotic solutions hold to a high degree of accuracy near the equator; likewise, near the poles, the exponential dependence of these solutions forces them to decay rapidly towards zero, in accordance with the behaviour of the numerical solutions dictated by the boundary conditions. Apart from a difference in sign for the  $\tilde{\Theta}$  functions, the prograde and retrograde  $s = 1$  Hough functions appear very similar, again highlighting the ability of the meridional order to represent the character of a given mode.

The Yanai modes, prograde and retrograde, also show good agreement between asymptotic and numerical results. For both these and the g modes, the waveguide boundaries lie interior to  $|\mu| = 0.3$ , which translates into a latitude  $\sim 20^\circ$ . Consistent with their definition, the boundaries fall at the points where both  $\hat{\Theta}$  is non-zero, and its second derivative vanishes. Furthermore, they are in approximate coincidence with the outermost extrema of  $\Theta$ , confirming the empirical finding of Bildsten et al. (1996) which was explained in the latter part of Section 3.1.

The waveguide boundaries for the Kelvin and r modes are located at much higher latitudes than those of the g and Yanai modes. Indeed, equation (42) formally gives  $\mu_{1/2} = 1.05$  for the r mode, such that it is not actually equatorially trapped. It is unsurprising, therefore, that the agreement between asymptotic and numerical Hough functions is very poor for this mode, especially towards the stellar poles. The situation is not quite so bad for the Kelvin mode, because a waveguide does exist; however, the asymptotic Hough functions differ sufficiently from zero at  $\mu = 1$  that they cannot be considered to fulfill the boundary condition imposed there.

As with the preceding section, a comparison of asymptotic and numerical results is facilitated through consideration of the relative error between them. In the present context, the error will be defined as

$$\Delta\Theta = \left\{ \frac{\int_0^1 [\Theta^{(a)} - \Theta^{(n)}]^2 d\mu}{\int_0^1 [\Theta^{(n)}]^2 d\mu} \right\}^{1/2} \quad (65)$$

for the  $\Theta$  Hough functions, and similarly for the  $\hat{\Theta}$  and  $\tilde{\Theta}$  functions; this definition provides a normalized measure of the root mean-square deviation between asymptotic and numerical results. Fig. 4 plots the error data  $\{\Delta\Theta, \Delta\hat{\Theta}, \Delta\tilde{\Theta}\}$  as a function of  $\nu$ , for the  $m = -2$ ,  $k = -2, \dots, 2$  modes considered previously.

The errors for the g-mode Hough functions decrease rapidly with increasing  $|\nu|$ , and is in reasonable agreement with the approximately-quadratic convergence suggested by the analysis of Section 3.1. Generally-speaking, the convergence is most rapid for the  $\Theta$  functions, and slowest for the  $\tilde{\Theta}$  functions. Similar behaviour is exhibited by the Yanai mode, if  $|\nu|$  is sufficiently large that it has the character of a g mode. The kink in the Yanai-mode  $\Delta\hat{\Theta}$  curve, at  $\nu \approx -3$ , arises because there the numerical eigenvalue  $\lambda^{(n)}$  passes through zero and becomes negative. As mentioned in the introduction, negative eigenvalues correspond to rotationally stabilized convective modes; because the asymptotic analysis neglected these modes, it is unsurprising that the Hough functions obtained through it, when  $\nu > -3$ , provide very poor representations of the exact tidal-equation solutions.

The convergence of the r- and Kelvin-mode asymptotic solutions lies somewhere between the linear rate predicted in Sections 3.1 and 3.2, and the quadratic rate found for the g and Yanai modes. Even by  $\nu = -10$ , the error for the r-mode Hough functions is greater than  $\sim 10$  per cent, further highlighting the fact that the asymptotic

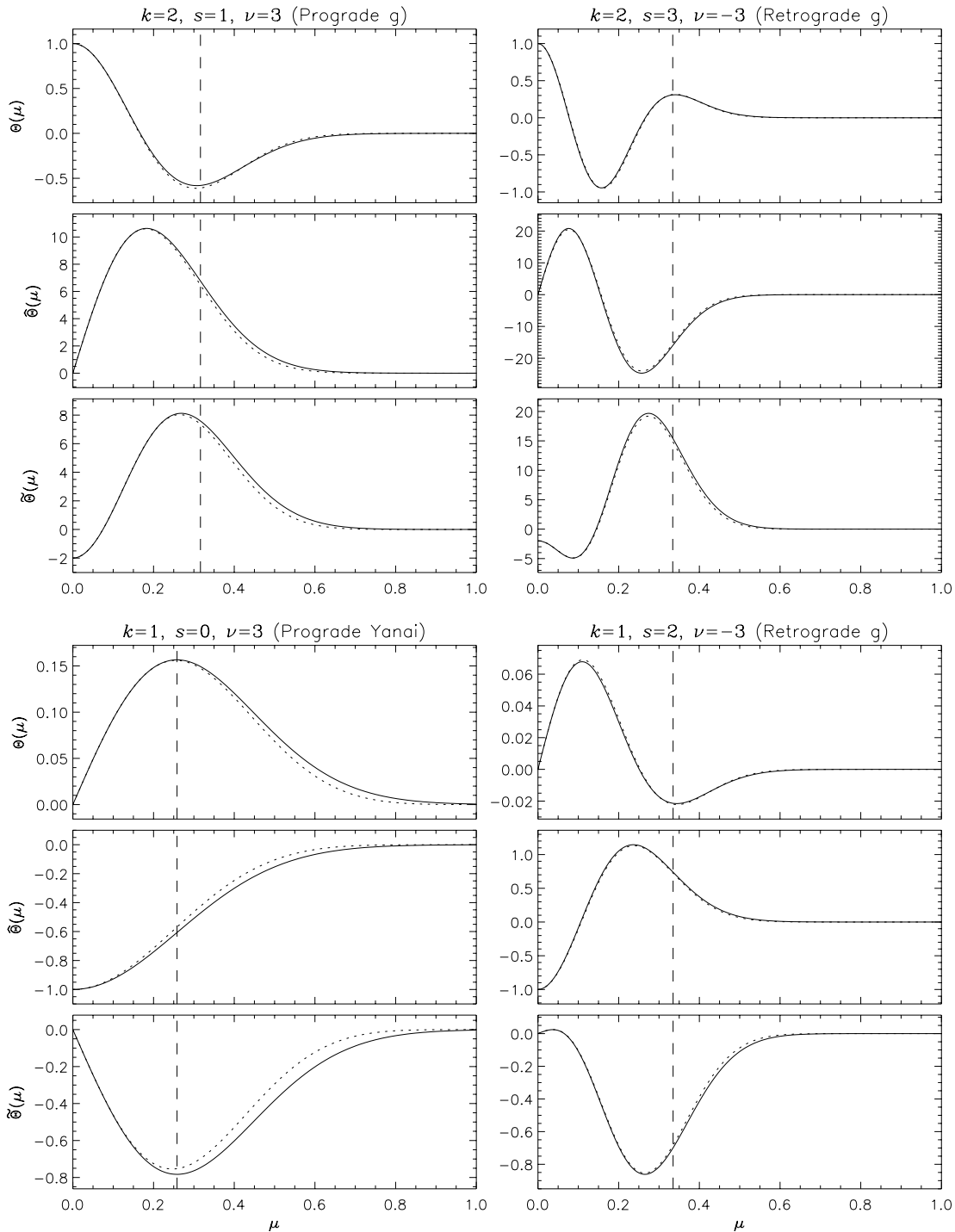


**Figure 3.** The asymptotic ( $\{\Theta^{(a)}, \hat{\Theta}^{(a)}, \tilde{\Theta}^{(a)}\}$ ; solid) and numerical ( $\{\Theta^{(n)}, \hat{\Theta}^{(n)}, \tilde{\Theta}^{(n)}\}$ ) Hough functions for  $m = -2, k = -2, \dots, 2$  modes, plotted as a function of the latitudinal co-ordinate  $\mu$  at selected values of the spin parameter  $\nu$ . In each case, the dashed vertical line indicates the location of the equatorial waveguide boundary.

approach is not good at reproducing these functions. The error is rather more acceptable for the Kelvin mode, dropping at  $\nu = 10$  to  $\sim 4$  per cent for the  $\tilde{\Theta}$  function, and to even less for  $\Theta$  and  $\hat{\Theta}$ .

## 6 DISCUSSION AND SUMMARY

In the preceding sections, analytical expressions for the Hough functions  $\{\Theta, \hat{\Theta}, \tilde{\Theta}\}$  were obtained, by solving approximate forms of

Laplace's tidal equations (18) and (21)–(22). These forms were derived by neglecting terms of order  $\mu^2$  (relative to those of the order of unity) in the equations – an approach pioneered, independently, by Matsuno (1966) and by Lindzen (1967), and since labelled the ‘equatorial beta-plane approximation’. This nomenclature originates from the definition  $\beta \equiv \Omega \sin \theta$  in the geophysical literature, representing the latitudinal derivative of the radial component  $\Omega \cos \theta$  of the rotation vector  $\Omega$ . The equatorial beta-plane

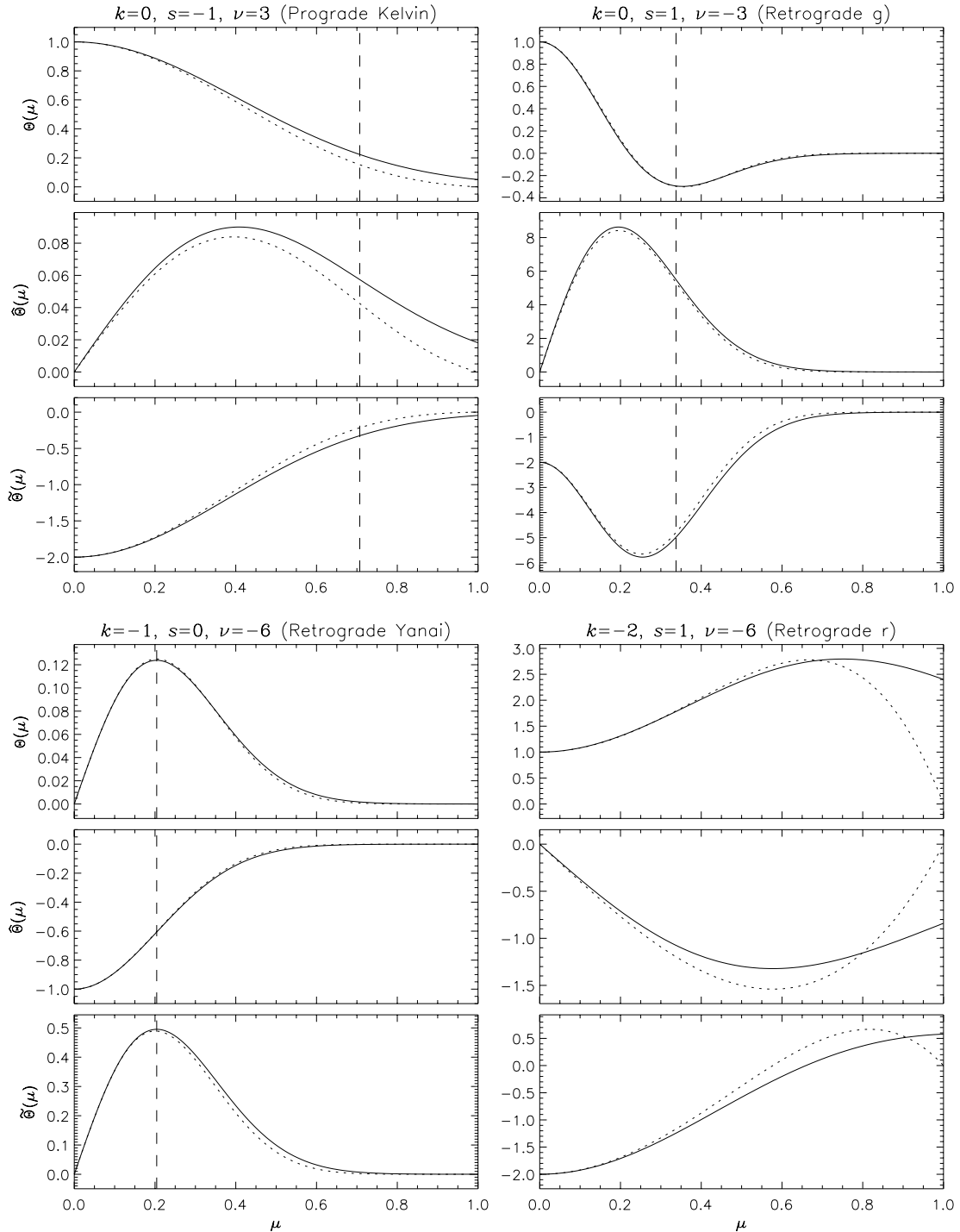


Figure 3 – continued

approximation refers to the assumption that  $\beta$  is constant (and equal to its equatorial value) across the Earth's surface, which is entirely equivalent to replacing by unity the  $(1 - \mu^2)$  terms in the tidal equations.

From the foregoing discussion, it is apparent that the asymptotic solutions found herein are familiar to those investigating terrestrial wave phenomena. However, these solutions are completely novel in an astrophysical context, which teaches a valuable lesson: that there exists a great body of knowledge in the domain of geophysics,

which is ripe for application towards the understanding of rotating-star nrp. Certainly, the two fields differ greatly in terminology and approach; nevertheless, the fundamental physical principles remain the same, and – as demonstrated herein – the problem of translating material from one field to the other is by no means insurmountable.

On more prosaic grounds, the utility of the asymptotic Hough functions rests, by one measure, on their ability to represent accurately the exact solutions to the tidal equations. Fig. 4 demonstrated that the  $g$ -mode functions fulfill this brief: even at values of the

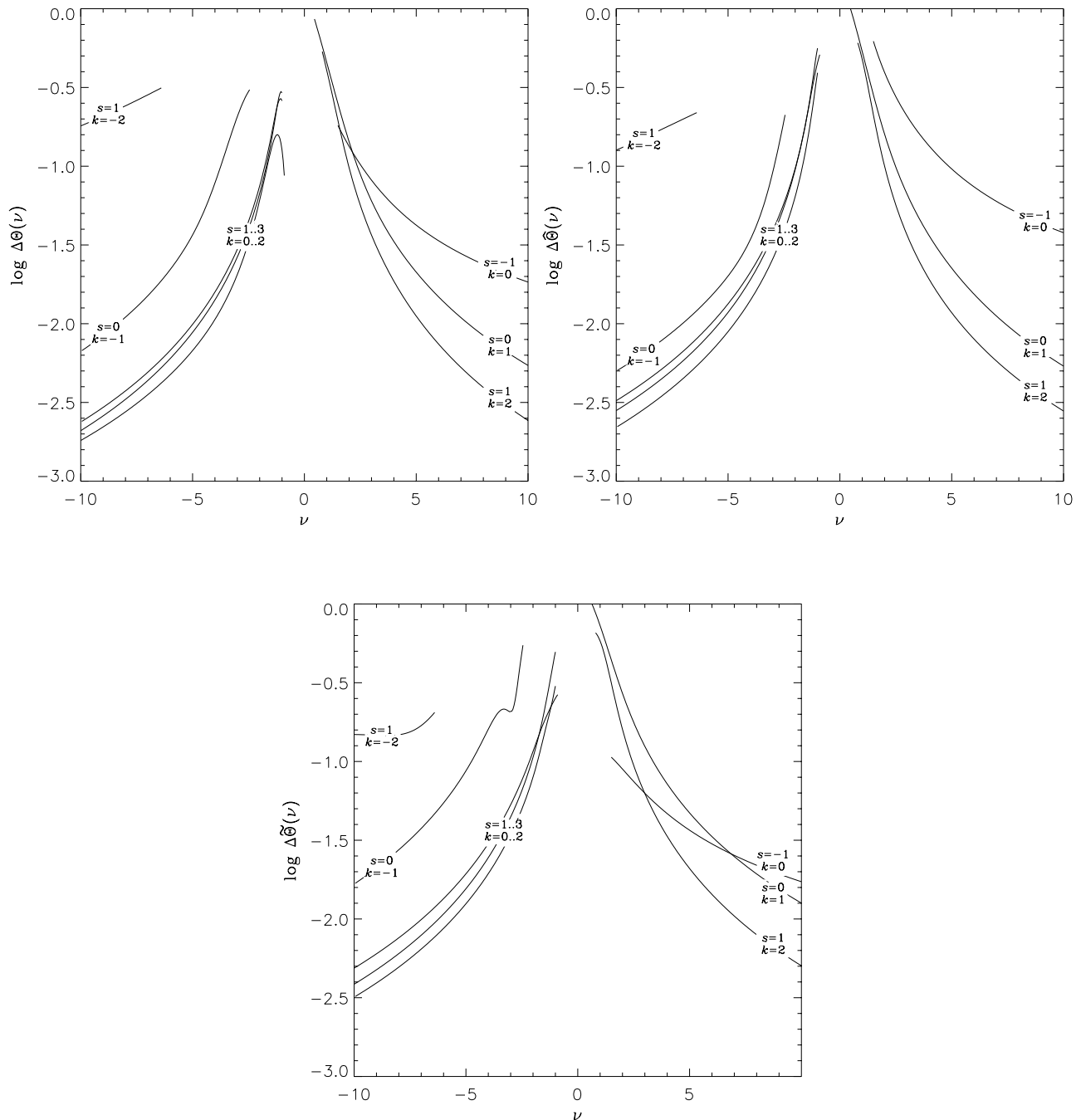


**Figure 4.** The relative error  $\{\Delta\Theta, \Delta\hat{\Theta}, \Delta\tilde{\Theta}\}$  between asymptotic and numerical Hough functions, plotted as a function of  $\nu$ , for  $m = -2$ ,  $k = -2, \dots, 2$  modes. Each curve is labelled by the appropriate  $k$  and  $s$  indices.

spin parameter as small as  $|\nu| = 2$ , they manage to reproduce well the exact solutions. However, the situation is less favourable for the other modes: the solutions for the Kelvin and Yanai modes only become accurate when  $|\nu|$  becomes large – in fact, larger than has ever been inferred from observations of pulsating stars. Furthermore, the convergence of the  $r$ -mode solutions is so poor that they are all but useless.

Nevertheless, to dismiss the asymptotic Hough functions on such grounds would miss a fundamental point: that they functions offer novel insights into  $n$ rp in rotating stars. One example is the recogni-

tion of prograde sectoral modes as instances of equatorially trapped Kelvin waves, which – unlike the  $g$  modes – owe their existence to the conservation of specific vorticity. This alternative propagation mechanism manifests itself in the behaviour of the Kelvin-mode eigenvalues  $\lambda$ , which change little with varying spin parameter (cf. equation 55), in contrast to the strong  $\nu$ -dependence exhibited by  $g$  modes (cf. equation 38).

Furthermore, the approximate expressions (43–44, 58) for the half-width of the equatorial waveguide may explain the long-standing conundrum of why prograde sectoral (i.e. Kelvin) modes

appear to dominate the line-profile variations of the rapidly-rotating  $\zeta$  Oph pulsators (see Unno et al. 1989). The half-width scales as  $\nu^{-1}$  for g modes, but as  $\nu^{-1/2}$  for the Kelvin modes. Therefore, at a given value of the spin parameter, the latter will reach appreciable amplitudes over a larger fraction on the stellar surface than the former, and should be easier to detect.

On a final note, the eigenvalues obtained through the asymptotic analysis are in themselves useful. As demonstrated towards the end of Section 4, these eigenvalues allow analytical dispersion relations to be obtained for the pulsation frequency  $\omega$ , which can be used to investigate how equatorially trapped modes transport energy and momentum in an azimuthal direction – possibly helping to clarify the rôle played by nrp in the disc-ejection episodes characteristic to Be stars (see e.g. Baade & Balona 1994). A follow-up paper is planned, to explore these issues.

#### ACKNOWLEDGMENTS

This work has been sponsored by the Particle Physics and Astronomy Research Council of the UK. I would also like to acknowledge valuable support from the Richard C. Lucas Foundation, and the use of NASA's Astrophysics Data System abstract service.

#### REFERENCES

Abramowitz M., Stegun I., 1964, Applied Mathematics Series 55, Handbook of Mathematical Functions. National Bureau of Standards, USA  
 Arfken G., 1970, Mathematical Methods for Physicists, 2nd edn. Academic Press, London

Baade D., Balona L. A., 1994, in Balona L. A., Henrichs H. F., Le Contel J. M., eds, Proc. IAU Symp. 162, Pulsation, Rotation and Mass Loss in Early-Type Stars. Kluwer, Dordrecht, p. 311  
 Bildsten L., Ushomirsky G., Cutler C., 1996, ApJ, 460, 827  
 Cowling T. G., 1941, MNRAS, 101, 367  
 Eckart C., 1960, Hydrodynamics of Oceans and Atmospheres. Pergamon Press, Oxford  
 Gill A. E., 1982, Atmosphere-Ocean Dynamics. Academic Press, London  
 Hough S. S., 1898, Phil. Trans. A, 191, 139  
 Lee U., Saio H., 1986, MNRAS, 221, 365  
 Lee U., Saio H., 1987, MNRAS, 224, 513  
 Lee U., Saio H., 1989, MNRAS, 237, 875  
 Lee U., Saio H., 1990, ApJ, 349, 570  
 Lee U., Saio H., 1997, ApJ, 491, 839  
 Lindzen R. S., 1967, Mon. Weath. Rev., 95, 441  
 Longuet-Higgins M. S., 1968, Phil. Trans. R. Soc. London, 262, 511  
 Matsuno T., 1966, J. Meteorol. Soc. Japan, 44, 25  
 Papaloizou J., Pringle J. E., 1978, MNRAS, 182, 423  
 Papaloizou J. C. B., Savonije G. J., 1997, MNRAS, 291, 651  
 Saio H., 1982, ApJ, 256, 717  
 Townsend R. H. D., 1997a, PhD thesis, Univ. of London  
 Townsend R. H. D., 1997b, MNRAS, 284, 839  
 Townsend R. H. D., 2000, MNRAS, 318, 1  
 Townsend R. H. D., 2003, MNRAS, in press  
 Unno W., Osaki Y., Ando H., Saio H., Shibahashi H., 1989, Nonradial Oscillations of Stars, 2nd edn. Univ. of Tokyo Press, Tokyo  
 Ushomirsky G., Bildsten L., 1998, ApJ, 497, L101  
 Yanai M., Maruyama T., 1966, J. Meteorol. Soc. Japan, 44, 291  
 Yoshida K., 1959, J. Oceanogr. Soc. Japan, 15, 159

This paper has been typeset from a  $\text{\TeX}/\text{\LaTeX}$  file prepared by the author.